Journal of Network Intelligence
Taiwan Ubiquitous Information
 ISSN 2414-8105 (Online)
Volume **8**, Number **4**, November **2023**

GCr15 Machining Tool Wear Based on Power Signals and Deep Learning Research

Bin Liu

School of Machinery and Transportation, Southwest Forestry University,
Kunming, China
1187848800@qq.com

Wei Li*

School of Machinery and Transportation, Southwest Forestry University,
Kunming, China
772074913@qq.com

Jun Wang

School of Machinery and Transportation, Southwest Forestry University,
Kunming, China
270254127@qq.com

Zhiwei Guo

School of Machinery and Transportation, Southwest Forestry University,
Kunming, China
594734792@qq.com

Xinyu Wei

School of Machinery and Transportation, Southwest Forestry University,
Kunming, China
1754587437@qq.com

Taiheng Wang

School of Machinery and Transportation, Southwest Forestry University,
Kunming, China
wthwsr@126.com

*Corresponding author: Wei Li

Received February 13, 2023, revised April 9, 2023, accepted June 18, 2023.

Abstract. *The magnitude of tool wear during the cutting process will affect machining quality and efficiency. This paper uses cutting power as a feedback signal and combines deep learning analysis to extract features to establish a cutting power monitoring system to monitor the tool wear status in real time. Experiments show that under the same cutting parameters, the cutting power increases with the increase of tool wear; and a deep learning-based monitoring model between cutting power and tool wear is established. The monitored wear value has a small error, and the tool wear can be monitored and predicted in real time while the machining is running continuously.*
Keywords: power signals, deep learning, tool wear, GCr15, experiments

1. **Introduction.** GCr15 steel is high-carbon chromium-bearing steel, heat-treated and processed with high hardness, high strength, good stability, and corrosion resistance [1], has good performance, and has been widely used. In today's smart manufacturing context, the most important thing is to achieve automation, intelligence, and continuous production of intelligent manufacturing systems, saving costs and improving efficiency while ensuring processing quality. The tool is the key component of the cutting process in smart manufacturing. Choosing various cutting parameters throughout the cutting process will result in varying degrees of tool wear, which will negatively impact the tool life and the processing quality of the parts [2]. When the cutting parameters and processing conditions are consistent, tool wear becomes a decisive factor in the change of the surface roughness of the workpiece [3]. When a tool wears reaches the threshold for failure, failing to replace the tool will affect the surface quality, and premature tool replacement can increase machining costs. Real-time tool wear monitoring may efficiently decrease the amount of downtime caused by tool wear and improve the efficiency of machining quality, preventing losses from tool wear [4]. Therefore, it is of great practical importance to obtain machining signals through effective detection means to judge and control tool wear in real-time during cutting and to take measures such as tool change or change of cutting parameters for process continuity and real-time control of workpiece quality in smart manufacturing, as well as tool wear control.

Tool wear detection techniques are classified as either direct or indirect depending on how they are observed [5]. The measurement accuracy is high [6], but the inspection equipment is not easily accessible to the cutting tool and the measurement accuracy is highly susceptible to external factors such as cutting fluid, chips, and light, and cannot provide continuous real-time process measurements. Therefore, direct measurement methods are not suitable for today's intelligent manufacturing systems that Pay attention to continuous processing. Indirect measurement refers to capturing physical signals related to tool wear, which are generated by the machine tool or tooling [7], such as vibration signals during machining [8], cutting force signals [9], acoustic emission signals [10], current and power signals [7] and other physical signals. Physical signals can be obtained without machine downtime, tool wear can be monitored in real-time and inspection data can be updated in real-time. However, the indirect detection method requires the installation of corresponding signal sensors in different locations of the machine tool, which also has certain limitations. Such as cutting force sensor devices need to be retrofitted for each machining process, the cost increases; vibration sensors due to safety factors, can only be installed at a certain distance from the spindle position, reducing the measurement accuracy; acoustic emission is sensitive to the impact of noise in the machining environment, the analysis is difficult.

In contrast, the power signal is considered to be one of the most suitable of the many detection signals for real-time tool wear detection. The power signal sensor is mounted on the power supply, does not affect the machining operation, and is not affected by factors such as cutting fluid. Therefore, real-time monitoring of tool wear during the cutting process using cutting power is a reasonable solution. Stavropoulos et al. [11] examined the correlation between power and vibration and tool wear and showed that power had a stronger correlation with tool wear than a vibration. Shao et al. [12] created a cutting power model for average return tool wear milling. To monitor tool wear, they used a power threshold method. Hassan et al. [13] proposed a generic multiple-signal fusion technique that uses raw spindle motor power, voltage, and torque signals to detect tool wear in real-time. Most studies have monitored tool wear by total power, while cutting power, which is directly related to tool wear, is only a small percentage of total power [14]. Few studies have examined the effect of tool wear on cutting power during machining. Therefore, this

paper establishes a cutting power monitoring system based on a deep learning algorithm for tool wear status by removing the power signals that are not relevant for tool wear detection from the total power, which reflects the tool wear status using the real-time fluctuation of cutting power during machine tool machining. Monitoring accuracy of tool wear can be improved by using this system, provide reference data for the selection of optimal cutting conditions and the optimization of cutting parameters, and provide technical support for reducing tool costs and ensuring the machining quality of workpieces.

2. Power models.

2.1. Machine power model.

Figure 1 illustrates how the power requirements for each stage of the machine tool's cutting process, including power on, spindle start, empty feed, cutting, empty feed, standby, and shutdown, vary. The two stages are the cutting stage and the non-cutting stage. The power of CNC machine tools is primarily standby power during the non-cutting stage, whereas the cutting stage's power signal is closely related to the machining parameters and tool wear.

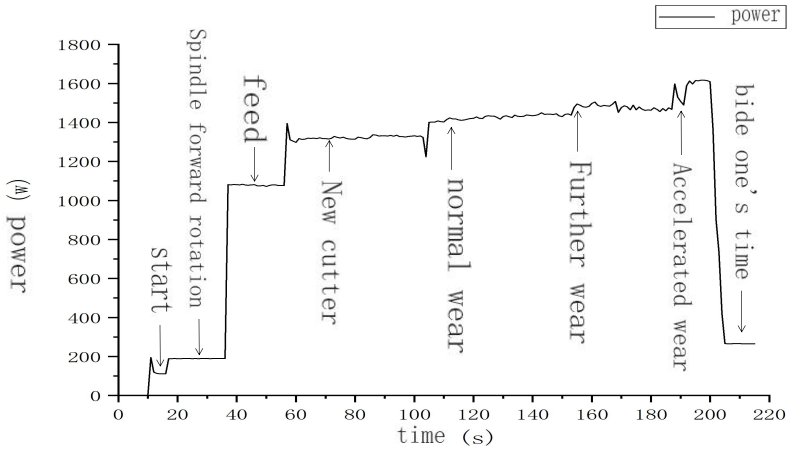

FIGURE 1. Cutting power variation diagram

The overall power of the machine tool can be broken down into the power of the cutting phase, the standby power, the spindle power, and the power of the process parameter as well as other powers from the perspective of the entire cutting process of the machine tool. The power gathered in this study represents the overall power used by the CNC machine tool when performing signal machining. The standby power, no-load power (P_n), and cutting power make up the machine tool's total power consumption (P_t) (P_c). P_t is the machine tool's overall power consumption and is equal to the sum of all other powers.

$$P_t = P_n + P_c \tag{1}$$

The cutting power P_c is related to the material of the workpiece and the depth of cut during the cutting process and is expressed as

$$P_c = PQ_r \tag{2}$$

where P is the theoretical cutting power and Q_r is the material removal rate.

The material removal rate, which to some part reflects the load on the machine tool during the cutting process [15], is the volume of material removed by the tool cutting in a unit of time. Q_r too much will accelerate tool wear and increase the load on the machine tool, The rate of material removal is expressed in terms of

$$Q_r = a_p a_e f_z z n \tag{3}$$

where a_p, a_e, and f_z are the cutting parameters; z is the number of teeth of the tool; n is the spindle speed.

In practice, the no-load power P_n is not influenced by the state of wear of the tool under the same cutting conditions, so the state of wear of the tool can be monitored more accurately using the power signal alone.

2.2. **Machining parameters and cutting power.** Cutting parameters have an impact on how cutting power varies, and cutting power and the variations in cutting speed, feed, and depth of cut are closely related, and the relationship between the cutting power P_c and the cutting parameters is

$$P_c = F_c V_c \tag{4}$$

where F_c is the cutting force, V_c is the cutting speed, and

$$V_c = \frac{\pi d n}{1000} \tag{5}$$

where V_c is the cutting speed, d is the diameter of the tool and n is the number of revolutions of the spindle.

Equation 5 can be expressed as

$$P_c = C_F a_p^{XF} V_c^{nF+1} K_F \tag{6}$$

Where a_p is the backdraft, f is the feed per revolution, C_F, XF, YF, nF, K_F Cutting force impact index.

It can be seen that as the cutting parameters change, the cutting power will change, as shown in equation 3. Therefore, the relationship between cutting power, machining parameters, and tool wear must be further investigated to detect tool wear, rather than just studying cutting power and cutting parameters.

2.3. **Cutting power and tool wear.** The cutting power of CNC machine tools increases in proportion to the amount of tool wear as the contact area between the tool and the workpiece expands from linear contact to surface contact. The more tool wear, the larger the direct contact area between the tool and the workpiece, the higher the contact friction between the two, and the greater the cutting power. Related research shows that tool wear generates cutting forces that can be expressed in two components

$$\begin{cases} F_{NW} = HVB * s \\ F_{FW} = \mu F_{NW} = \mu HVB * s \end{cases} \tag{7}$$

F_{NW} is the radial force by the tool, F_{FW} is the frictional force, H is the workpiece hardness, VB is the amount of wear on the rear tool face, μ is the coefficient of friction and s is the length of the war zone on the rear tool face.

As a result, the cutting power due to tool wear can be expressed as

$$P_c = F_{FW} V_c = \mu HVB * s V_c \tag{8}$$

where V_c is the cutting speed.

The formula for the correlation between tool wear and cutting power is

$$VB = \frac{P_c}{\mu H * s V_c} \tag{9}$$

3. **Signal acquisition systems for deep learning.** Deep learning is a deep structural model based on neural network algorithms. In the field of tool wear monitoring, models based on deep learning with power data processing and feature extraction capabilities and high monitoring accuracy are used extensively. A convolutional neural network in a deep learning model is used to monitor tool wear in this paper.

3.1. **Power signal acquisition and pre-processing.** The current research process for monitoring and predicting tool wear can be divided into steps including signal capture, data preparation, feature extraction, and model construction. The specific method is to use a power collector to collect the relevant signals through different cutting parameters, remove the influencing factors and then use deep learning to extract the signal features and build a model to achieve the purpose of wear state identification. The specific process is shown in Figure 2.

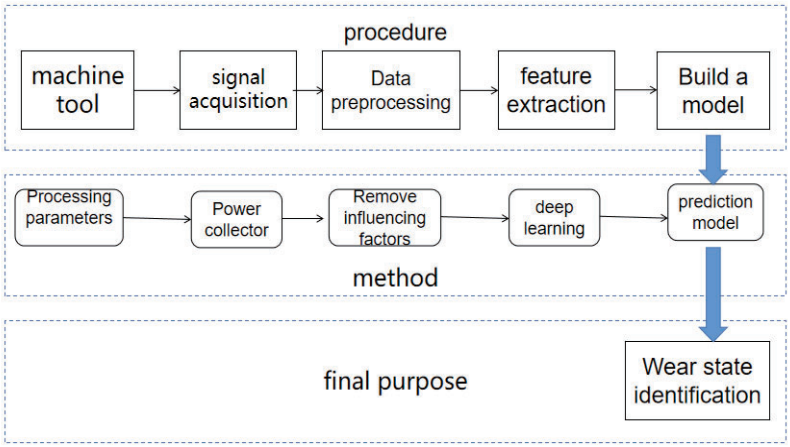

FIGURE 2. Tool wear model building process

In terms of the tool wear process, There are three stages of tool wear: initial wear, normal wear, and rapid wear [16]. To monitor the tool wear state at different stages by the change of the power signal, a signal acquisition system was set up, as shown in Figure 3, consisting of two modules, a hardware part, and a software part. Identifying and predicting tool wear is the ultimate goal.

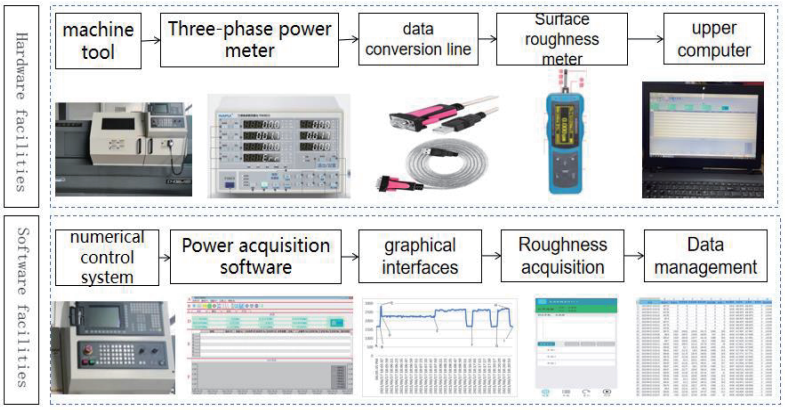

FIGURE 3. Power signal acquisition system

The external environment interferes with the data collected by the power signal acquisition system. The collected power signals need to be pre-processed to improve the quality of the acquisition, the accuracy of the calculation and to ensure accurate extraction of the tool wear condition characteristics. The invalid signals at the beginning and end of the data are removed and the maximum value is set to a threshold value, keeping only the valid cutting power data.

3.2. **Deep learning to extract signal features.** During the cutting operation, a power sensor records the cutting power signal. A deep learning technique is then used to extract the signal characteristics of the cutting power. The data is then downscaled to produce the cutting power's energy spectrum as input to the model [17, 18, 19, 20]. After each cut, the tool is passed through a microscope to observe and measure the wear on its back face, and the measured wear data is also input into the model. The tool wear is processed by the convolution kernel in the convolution layer to generate a feature curve, which is compressed by the pooling layer and fed into the fully connected layer for wear classification. Tool wear monitoring and prediction can be achieved by feeding the real-time power signal into the model. Figure 4 shows the basic process of tool wears monitoring based on the deep learning model.

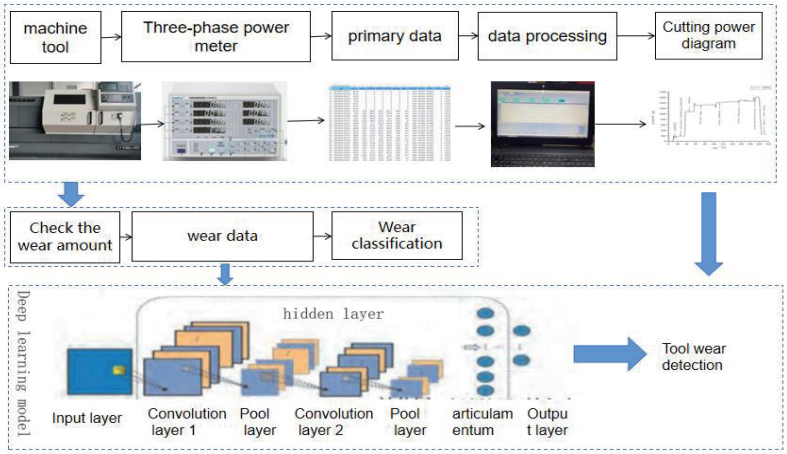

FIGURE 4. Deep learning process diagram

An iteration of the cutting tool signal features and their extraction results can be expressed as

$$\begin{cases} C_q = \frac{\sum_{i=1}^{n}(|xi|-\bar{X})^4}{\bar{X}} \\ C_f = \frac{X_{\max}}{\bar{x}} \\ C_e = \frac{x_{\max}}{x_f} \end{cases} \tag{10}$$

where C_q, C_f, and C_e are the signal cliff factor, pulse factor, and margin factor of the cutting tool respectively; n is the number of extracted features; X_{rms} is the root mean square of the signal; xi is the input sample signal; X_i, $X_{\max}$, X_r are the mean, maximum and root square amplitude of the sampled signal respectively.

The frequency characteristics of the tool during the cutting process are expressed as

$$fz = \frac{Ns}{60} \tag{11}$$

where Ns is the spindle speed.

The amplitude spectrum, phase spectrum, and power spectrum are also frequency domain features of the cutting tool signal and can be calculated by the Fourier transform. Based on this, the feature extraction results are dimensionalized using a deep learning algorithm, and the average activation of the j-th node on the hidden layer in the deep confidence network is defined as

$$\rho_j = \frac{1}{n}\sum_{i=1}^{n} h_j\,(xi) \tag{12}$$

where $h_j\,(xi)$ is the activation function of the corresponding feature of signal xi.

To ensure that the calculated ρ_j does not deviate from the sparsity parameter, a sparsity penalty factor is added to the cost function and the initial features are fed into the deep learning algorithm, resulting in a final result that is the dimensionality reduction of the tool cutting power signal features.

4. Cutting experiments.

4.1. Experimental platform construction.

To study the cutting power signal for tool wear monitoring, an experimental platform was built to support the study based on the cutting power acquisition system, as shown in Figure 5. A CNC lathe manufactured by Yunnan Machine Tool Factory is used in the system, and the built cutting power monitoring system (PM9833A three-phase power monitor, signal converter, CNC lathe, and host computer from Dongguan Nap Electronic Technology Co. The three-phase power monitor collects the signals of voltage, current and active power of the CNC lathe under different cutting parameters, converts them into digital signals, and transmits them to the upper computer for data recording. The test object chosen for the study was a YT15 carbide tool, consisting of an insert and a tool holder, with the same tool holder and using different tools for an experiment. To avoid other factors affecting the results, the tools were initially tested as new and without surface wear.

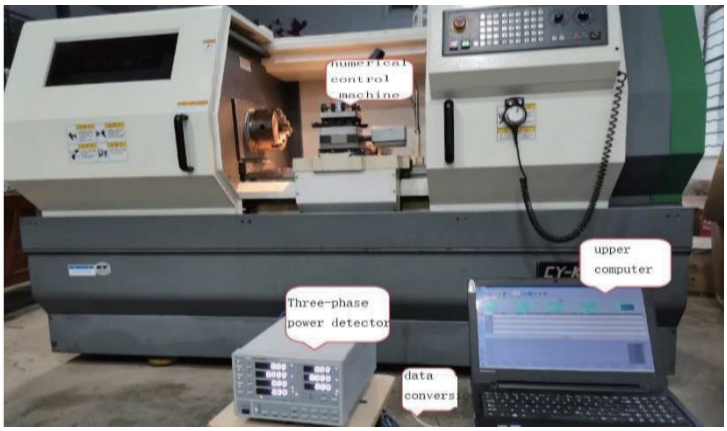

FIGURE 5. Experimental system

4.2. Experimental design.

During the cutting process, the PM9833A three-phase power monitor mounted on the machine's power supply selects the voltage signal, the current signal, and the power as the sampling signals, with an integration sampling frequency of 1 second/time. The tool wear value after each cut was observed and measured using an optical microscope, and the average value of the cutting force was extracted in the time domain. Four factors were selected as experimental variables in the experiment, namely cutting speed, depth of cut, feed, and tool wear. The experiments were conducted separately with four level values of the single factor group. The first group was a univariate experiment with cutting speed at tool wear of 0.0386mm, depth of cut of 0.1mm, and feed of 0.1; the second group was a univariate experiment with depth of cut at cutting speed of 60m/min and feed of 0.125mm; the third group was a univariate experiment with cutting speed of 70m/min, wear of 0.0386mm and univariate analysis of the depth of cut.125mm with 0.0386mm tool wear; the third group was a univariate experiment with 70m/min cutting speed, 0.0386mm wear and univariate analysis of the depth of cut at 70m/min cutting speed and 0.1mm depth of cut. The fourth, fifth, and sixth groups of experiments

were univariate experiments with a cutting tool with 0.1537mm wear, and the experimental variables were the same as the first, second, and third groups; the seventh, eighth, and ninth groups were repeated univariate experiments with a tool with 0.3235mm wear, and the experimental variables were the same as the first, second and third groups. The four factors mentioned above will be studied separately for their influence on the cutting power signal, and the collected power signal will be used as the research object. The results of single factor experiments are shown in Table 1.

Table 1. Results of the one-way experiment

No.	Amount of wear and tear (mm)	Cutting speed (m/min)	Depth of cut (mm)	Feeds	Total power	No-load power	Cutting power
1	0.0386	50	0.1	0.1	1194.82	892.17	302.65
2		60			1318.73	966.95	351.78
3		70			1427.46	972.12	455.34
4		60	0.1	0.125	1324.01	962.3	361.71
5			0.15		1332.46	952.85	379.61
6			0.2		1341.16	947.34	393.82
7		70	0.2	0.1	1448.36	963.26	485.1
8				0.125	1460.84	972.47	488.37
9				0.15	1462.47	970.09	492.38
10	0.1537	50	0.1	0.1	1259.77	892.07	367.7
11		60			1428.61	935.15	493.46
12		70			1561.03	998.69	562.34
13		60	0.1	0.125	1438.98	958.34	480.64
14			0.15		1463.7	958.64	505.06
15			0.2		1490.48	965.4	525.08
16		70	0.2	0.1	1538.44	1001.31	537.13
17				0.125	1565.9	976.46	589.44
18				0.15	1567.89	970.95	596.94
19	0.3235	50	0.1	0.1	1344.41	892.07	452.34
20		60			1484.09	902.11	581.98
21		70			1531.98	892.72	639.26
22		60	0.1	0.125	1406.84	898.12	508.72
23			0.15		1422.46	847.64	574.82
24			0.2		1439.85	853.73	586.12
25		70	0.2	0.1	1608.43	988.97	619.46
26				0.125	1610.45	978.62	631.83
27				0.15	1611.28	967.58	643.7

4.3. **One-factor experiment analysis of results.** The cutting power variation curve based on the data in Table 1 is depicted in Figure 6. A single-factor experiment was conducted to determine the average total power consumed by the tool at various cutting parameters.

As can be seen from Figures 6A, 6B, and 6C, the greatest impact of cutting speed on power is observed. The total power consumed by the machine tool increases with the rise in depth of cut, machining efficiency rises with the rise in feed, and the total power consumed by the machine tool increases with the rise in cutting speed for the same amount of tool wear.

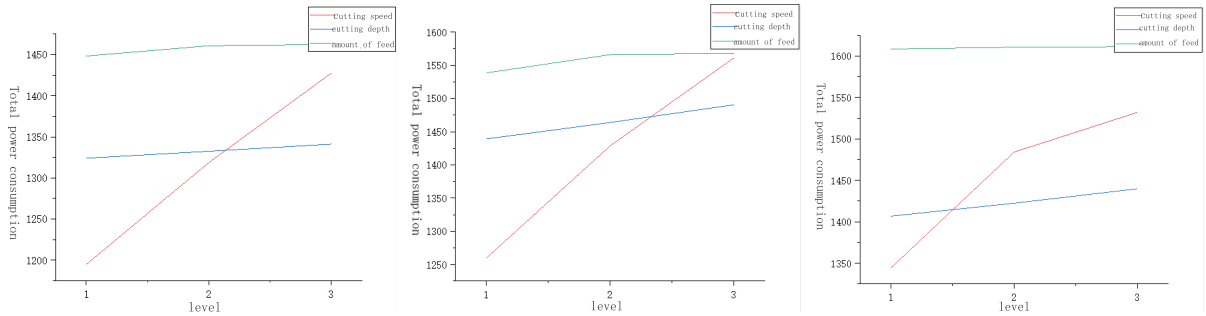

(A) Tool wear 0.0386mm (B) Tool wear 0.1537mm (C) Tool wear 0.3235mm

FIGURE 6. Variation of the effect of tool wear on the total power consumed

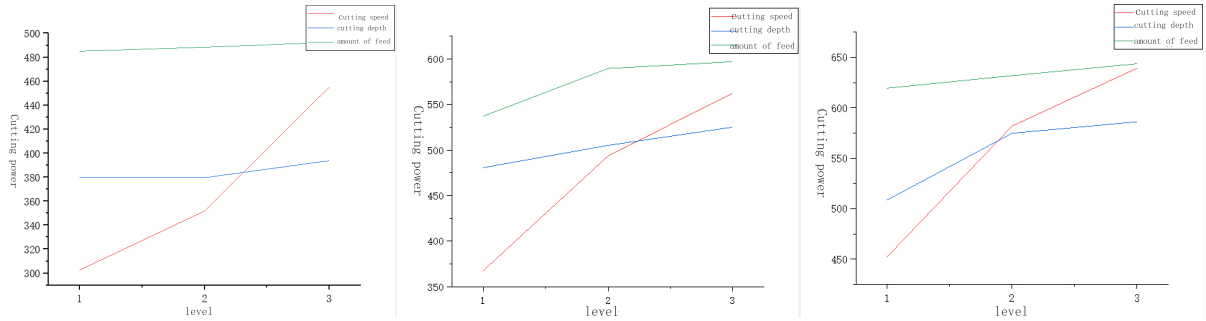

(A) Tool wear 0.0386mm (B) Tool wear 0.1537mm (C) Tool wear 0.3235mm

FIGURE 7. Graph showing the effect of tool wear on cutting power

From Figures 7A, 7B, and 7C can be seen, in addition to the influence of no-load power on. In different tool wear situations, the cutting power change law and the total power change law will remain the same, and the cutting power change will be more obvious. With the cutting speed of 50 $\sim$ 70 m/min increase, the cutting performance followed by a significant increase, the cutting speed of 70 m/min cutting performance is the largest; With the increase in feed, cutting power slowly rises, that cutting power by the feed increase in the impact of less; With the cutting depth increases, cutting power increases the smallest, that cutting power by the cutting depth increases the smallest impact. According to the above analysis: cutting parameters in the three factors on the impact of cutting power, cutting speed is the largest, the feed amount is the second, and the depth of cut is the smallest.

4.4. **Analysis of orthogonal test results.** To compensate for the shortcomings of the single-factor experimental method, orthogonal experiments were designed to investigate the variation of cutting performance under the influence of four factors in combination with the actual process parameters. Table 2 shows the results of the orthogonal experiments.

As shown in Figure 8A, the total power is smallest and increases quickly at 0.0386 mm tool wear; it increases steadily at 0.1537 mm tool wear; and it is largest and increases rapidly at 0.3235 mm tool wear. As tool wear increases, so does cutting performance. The basic rule is the same as the rule of variation between tool wear in single-factor experiments. It can be seen that cutting parameters and tool wear together to affect the cutting performance, with cutting speed > feed >depth of cut in the order of influence. Both cutting parameters and tool wear to increase the cutting performance and the trend is consistent with the single-factor effect.

TABLE 2. Table of factor levels for orthogonal experiments

No.	Amount of wear and tear (mm)	Cutting speed (m/min)	Depth of cut (mm)	Feeds	Total power	No-load power	Cutting power
1	0.0386	50	0.1	0.1	1329.8	1041.3	288.5
2	0.0386	60	0.15	0.125	1401.85	997.52	404.33
3	0.0386	70	0.2	0.15	1477.46	988.74	488.72
4	0.1537	50	0.1	0.1	1337.89	979.21	358.68
5	0.1537	60	0.15	0.125	1443.43	947.85	495.58
6	0.1537	70	0.2	0.15	1548.42	965.09	583.33
7	0.3235	50	0.1	0.1	1343.33	914.56	428.77
8	0.3235	60	0.15	0.125	1448.17	932.2	515.97
9	0.3235	70	0.2	0.15	1608.13	986.73	621.4

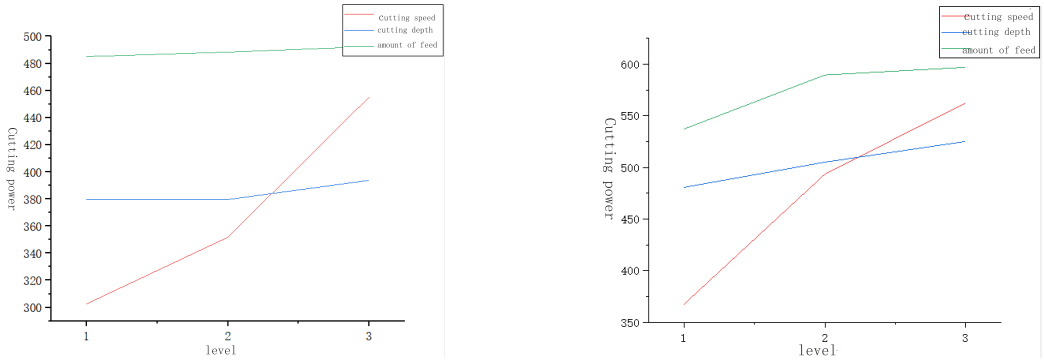

(A) Effect of total power consumption (B) Effect on cutting power

FIGURE 8. Effect of orthogonal experimental factors on power

5. **Analysis of cutting power and tool wear.**

5.1. **Tool wear Analysis.** The dulling standard for carbide tools specifies a wear amount of 0.3mm on the rear face of the tool [3]. Because the amount of wear generated by the tool's interaction with the workpiece during machining is very small and cannot be measured with the naked eye or conventional methods, a 3D digital microscope was used in this experiment to measure and read the wear area and size of the wear on the tool's rear face. Figure 9 depicts the tool's wear at 0.0386mm, 0.1537mm, 0.2605mm, and 0.3235mm.

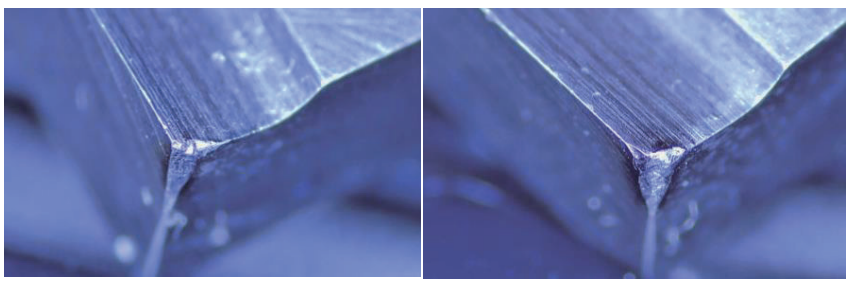

c Tool wear of 0.2605 mm d Tool wear of 0.3235 mm

Figure 9a depicts the tool's initial wear stage (wear amount 0.0386mm): The contact area between the tool and the workpiece surface is tiny at this stage, and the cutting force is focused in the tooltip region, the tool surface will fall off quickly, the friction

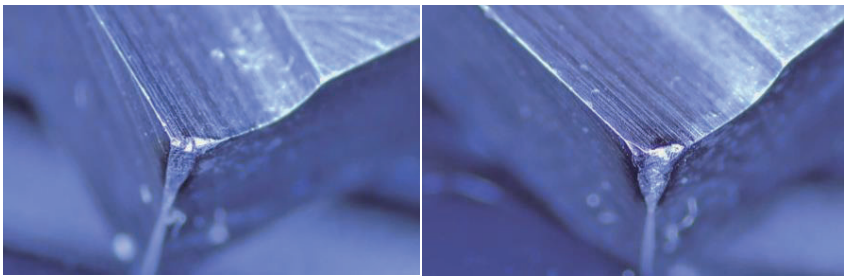

c Tool wear of 0.2605 mm d Tool wear of 0.3235 mm

FIGURE 9. Graph showing wear of different tools

between the tooltip and the machining surface forms abrasive wear, also in the case of high-temperature forms bonded wear; Figure 9b shows the normal wear stage of the tool (wear amount 0.1537mm): Currently, the tool and the job The contact area expands, tool wear decreases, wear is more uniform, and cutting power grows more smoothly.

Figure 9c shows the rapid wear stage (wear amount 0.2605mm): when the tool wear amount rises to a certain level, the rate of wear will rise rapidly, resulting in a rise in the surface roughness of the workpiece, a drop in cutting quality and a rapid rise in cutting power; Figure 9d has a wear amount of 0.3235mm: more than 0.3mm above the tool wear standard. At this stage the surface roughness of the workpiece drops significantly, affecting workpiece quality, generating tool tremors, cutting power as well as cutting temperature is extremely unstable. The entire tool wear process is shown in Figure 10, where the instrument goes through three stages of wear to meet the wear standard: beginning wear, regular wear, and accelerated wear.

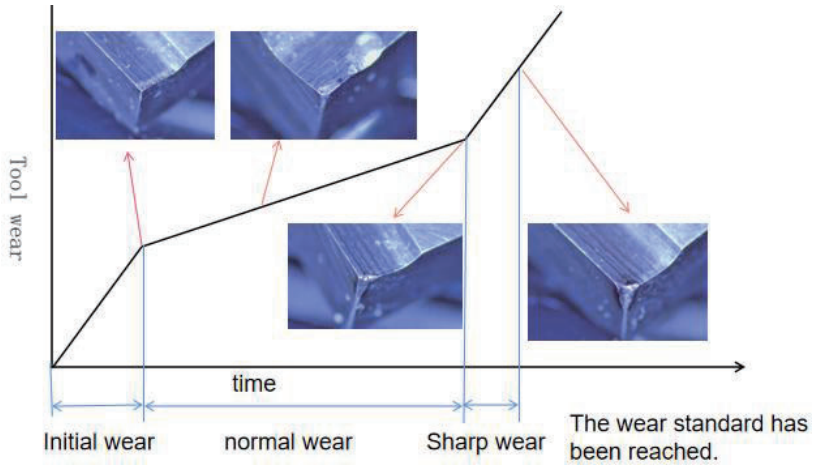

FIGURE 10. Typical curve of tool wear

5.2. **Effect of tool wear on cutting power.** The power detector can monitor signal characteristics such as three-phase electrical voltage, current, active power, reactive power, and apparent power without changing the structure of the machine tool itself and at a cheaper cost than other signal collection equipment. The power signal is gathered using a deep learning analysis and processing system, which first analyzes the whole power signal of the machine tool, then removes no-load power, obtains cutting power directly connected to tool wear, and improves signal accuracy.; the power data will be imported into the deep learning model to learn, analysis and extraction of different signal features reflecting different tool wear amount, to achieve the purpose of monitoring and predicting

tool wear. The power monitoring system is far more convenient and cost-effective than other monitoring systems in use and does not affect the continuity of the machining system. Single-factor and orthogonal experiments were carried out to collect the relevant power signal data, and the effect of tool wear on cutting the power after processing is shown in Figure 11.

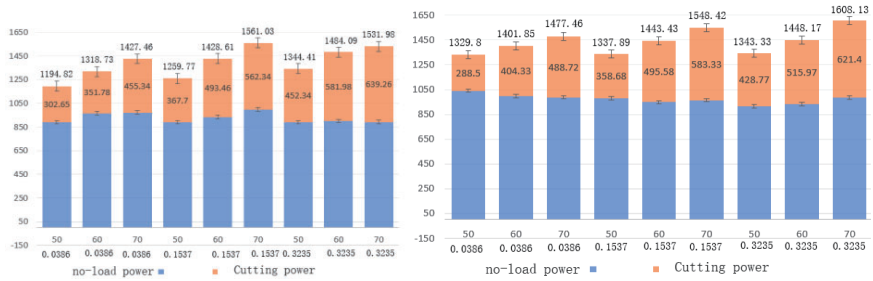

a One-factor experiment b Orthogonal experiment

FIGURE 11. Curve of the effect of tool wear on cutting power

As shown in Figure 11, experiments were carried out at cutting depths of 0.1mm and feeds of 0.1, and at cutting speeds of 50m/min, 60m/min, and 70m/min respectively. The experiments showed that the cutting power was lowest at a cutting speed of 50m/min and increased with wear, from 302.65w to 452.34w; at a cutting speed of 60m/min, the increase in cutting power slowed down, from 351.78w to 581.98w; at a cutting speed of 70m/min, the increase in cutting power slowed down further, from This indicates that the cutting power is greatest at a cutting speed of 70m/min with the same amount of wear and that the cutting power increases with the increase in cutting speed. Under the same cutting parameters, with the rise of tool wear, cutting power increases with the increase of tool wear, tool wear, and cutting power are positively correlated.

5.3. **Predictive model for cutting power on tool wear.** According to an examination of the experimental data, as tool rear face wear grows, so does the amount of contact between that surface and the workpiece, which in turn raises friction force and, eventually, cutting power. Deep learning algorithms are used in the prediction process to learn from the experimental data. Data on tool wear and cutting power obtained from the experiments are evaluated, features are extracted and dimensionality is reduced and transformed to obtain a power spectrum map, which is used as input to the model in deep learning. Tool wear is processed through a convolution layer, feature curves are generated, input to the connectivity layer, and wear is classified. When the real-time cutting power signal is fed into the predicting model, real-time tool wears monitoring and prediction can be achieved. A cutting power-based tool wear prediction model is developed. The following equations are used.

$$VB_{rt} = -0.154 + 4.4 \times 10^{-4} P_c + 4.28 \times 10^{-7} P_c \tag{13}$$

where VB_{rt} is the real-time tool wear value during tool cutting and P_c is the real-time cutting power.

5.4. **Experiment.** Experiments were conducted to validate the tool wear prediction model developed in section 4.3 and to confirm its correctness. The data was analyzed using the deep learning method in 2.2 after the power signal was obtained by the collection mechanism of 2.1 and the tool wear was measured under a microscope. Figure 12 depicts the ultimate cutting power fluctuation, whereas Figure 13 depicts the tool wear variation.

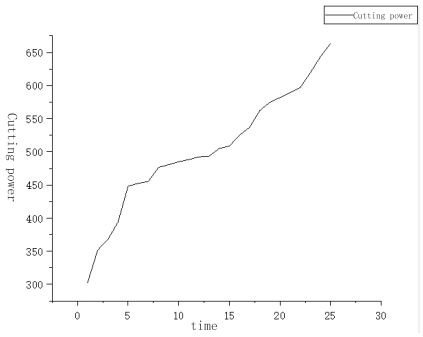

FIGURE 12. Cutting power variation curve

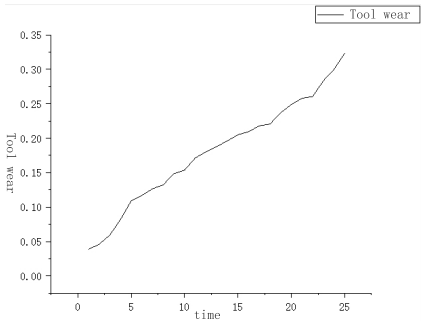

FIGURE 13. Tool wear variation curve

The tool wear variation curve likewise goes through three stages quick rise, slow rise, and sharp rise, in line with the traditional tool wear variation curve, as illustrated in Figures 12 and 13. The cutting power curve exhibits three stages of rapid rise, slow rise, and rapid rise with cutting time.

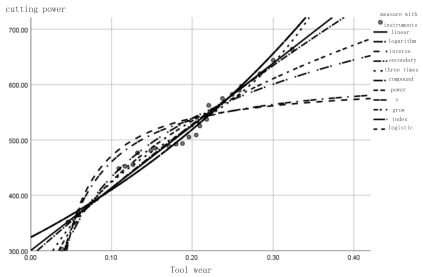

FIGURE 14. Regression analysis

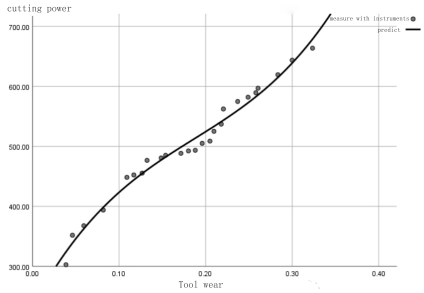

FIGURE 15. Fitting curv- e of cutting power and tool wear

Regression analysis was performed on cutting performance and tool wear as shown in Figure 14, and analyzed linearly, logarithmically, and exponentially. The final fit was made to the cutting performance and tool wear. Analysis of the fitted curves for the measured and predicted values of cutting power and tool wear, as shown in Figure 15, shows that the measured and predicted values are within a small error and are very precise.

6. **Conclusion.** To regulate machining quality while lowering safety risks and quality expenses resulting from tool wear, it is necessary to detect tool wear in real-time. In this paper, a cutting power monitoring system is established using cutting power and deep learning techniques. The system can receive the cutting power signal of the machine tool being used in production in real time as a feedback signal, analyze the signal using deep learning to extract features, and then use the features to monitor and forecast tool wear in real-time.

As the cutting parameters increase, the machine's overall power consumption rises. The cutting speed has the greatest impact on this power variation, followed by the feed and the depth of the cut. Cutting power is influenced by both cutting parameters and tool wear, and fixed cutting parameters can be used to track and anticipate tool wear based on cutting power. The established cutting power-based tool wear model has been validated experimentally to show that the prediction model has low prediction error and high accuracy. The system provides real-time information on tool wear and parameters

during machining and timely replacement of worn tools, providing technical support for workpiece machining quality.

Future research will focus on the use of cutting power signals or the deep integration of multi-signal fusion and depth algorithms to enable more accurate and faster tool wear monitoring results and accurate prediction of tool life.

REFERENCES

[1] Y.-N. He, S.-R. Yu, X.-S. Li, C. Shao, and Q. Chen. "Motion distribution of micro-motion wear particles of TC4 alloy." *Rare Metal Materials and Engineering*, vol. 49, no. 4, pp. 1250–1255, 2020.

[2] C.-B. Li, T. Wan, X.-Z. Chen, and Y.-F. Lei."Online monitoring of tool wear for CNC turning batch machining based on cutting power." *Computer Integrated Manufacturing Systems*, vol. 24, no. 8, pp. 1910–1919, 2018.

[3] M.-H. Wang, D.-L. Zhou, Y.-H. Zheng, C.-F. Shao, and X. Zhuang. "Milling test and wear analysis of TA15 titanium alloy." *Tool Technology*, vol. 52, no. 3, pp. 109-112, 2018.

[4] Y. Lin, S.-Y. Gao, T.-S. Liu, and K.-P. Zhu. "A deep learning-based method for predicting the wear state of high-speed milling tools." *Mechanics and Electronics*, vol. 35, no. 7, pp. 12-17, 2017.

[5] L.-H. Zhao, J.-C. Zhang, and S.-R. Ning. "Experimental study of micro-miniature tool wear detection based on machine vision." *Manufacturing Automation*, vol. 34, no. 10, pp. 53-56, 2012.

[6] Y. Fu."Research on intelligent monitoring technology for vibration state and tool wear during cutting machining." *Ph.D. Huazhong University of Science and Technology*, 2017.

[7] Y.-F. Gui, W.-Guan, B.-Chen, and B.-Shen. "Online monitoring of tool wear status based on HHT algorithm and spindle power signal." *Machine Design and Research*, vol. 35, no. 5, pp. 63-69, 2019.

[8] M. Wang, Y.-P. Li, J.-S. Hou, and B. Yang. "Experimental study on the wear law of coated milling cutters considering current and vibration." *Machine Manufacturing and Automation*, vol. 48, no. 5, pp. 13-16, 2019.

[9] M.-H. Xiao, N. He, and L. Li. "Studies on tool wear monitoring based on cutting force //Materials Science Forum." *Trans Tech Publications Ltd*, vol. 69, no. 7, pp. 268-272, 2012.

[10] Z.-F. Zhou, D. Hong, and C.-J. Huang. "Research on online monitoring of tool wear status based on acoustic emission signal analysis." *Tool Technology*, vol. 56, no. 12, pp. 51-55, 2022.

[11] P. Stavropoulos, A. Papacharalampopoulos, E. Vasiliadis, and G. Chryssolouris. "Tool wear predictability estimation in milling based onmulti- sensorial data." *The International Journal of Advanced Manufacturing Technology*, vol. 82, no. 1-4, pp. 509-521, 2016.

[12] H. Shao, H.-L. Wang, and X.-M. Zhao. "A cutting power model for tool wear monitoring in milling." *International Journal of Machine Tools and Manufacture*, .vol. 44, no. 14, pp. 1503-1509, 2004.

[13] M. Hassan, A. Sadek, and M.-H. Attia. "Intelligent machining: real-time tool condition monitoring and intelligent adaptive control systems." *Journal of Machine Engineering*, vol. 18, no. 1, pp. 5-17, 2018.

[14] H.-S. Yoon, J.-Y. Lee, M.-S. Kim, and S.-H. Ahn. "Empirical power-consumption model for material removal in three-axis milling." *Journal of Cleaner Production*, vol. 78, pp. 54-62, 2014.

[15] Y.-Z. Cheng. "ACIS-based Five-Axis Milling Simulation and Material Removal Rate Optimization Research." MA thesis. Huazhong University of Science and Technology, 2012.

[16] L.-B. Guo. "technology of metals ." *Shandong Science and Technology Press*, 2008.

[17] Y.-R. Ma, Y.-J. Peng, and T.-Y. Wu,"Transfer learning model for false positive reduction in lymph node detection via sparse coding and deep learning." *Journal of Intelligent & Fuzzy Systems*, 2022 (Preprint): 1-13.

[18] C.-M. Chen, S. Lv, J. Ning, and J.-M. Wu. "A Genetic Algorithm for the Waitable Time-Varying Multi-Depot Green Vehicle Routing Problem." *Symmetry*, vol. 15, no. 1, pp. 124, 2023.

[19] M.-E. Wu, J.-H. Syu, and C.-M .Chen. "Kelly-based options trading strategies on settlement date via supervised learning algorithms." *Computational Economics*, vol. 59, no. 4, pp. 1627-1644, 2022.

[20] V.-Kumar, R.-Kumar , V.-Kumar , and S.-Kumari. "RAVCC: Robust Authentication Protocol for RFID based Vehicular Cloud Computing." *Journal of Network Intelligence*, vol. 7, pp. 526-543, 2022.